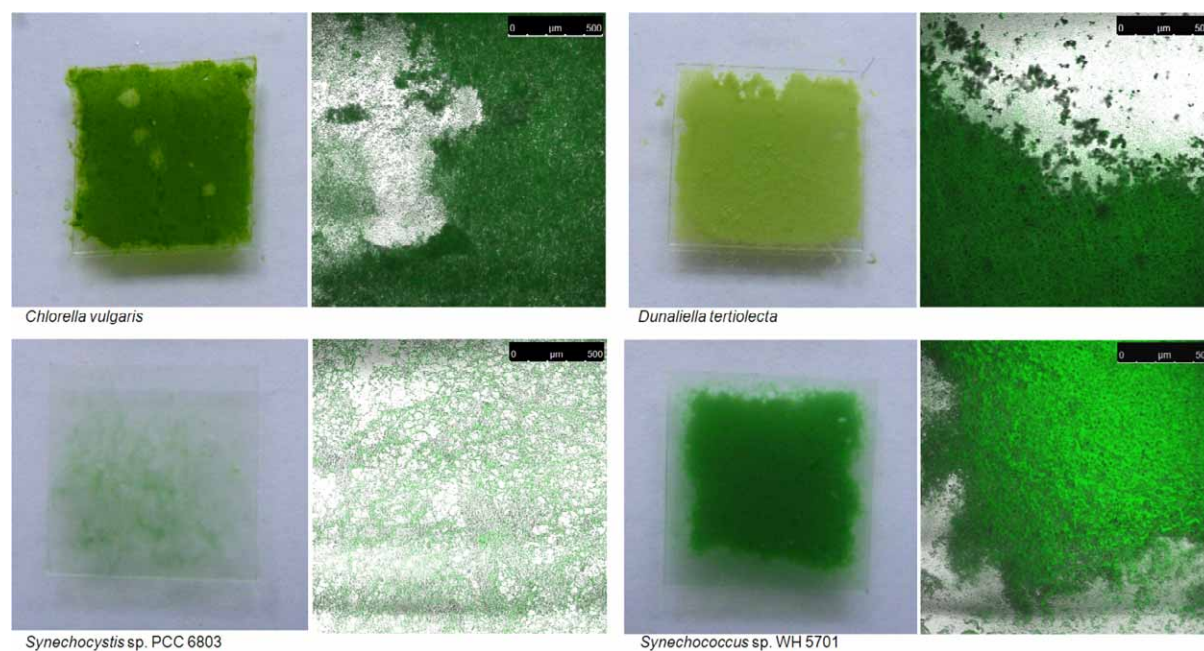


**Supp. Table 1. Media conductivity**

Each media (approximately 5 ml) was measured at a reference temperature of 25°C. The conductivity of filter-sterilized sea water and deionised water are included as reference points.

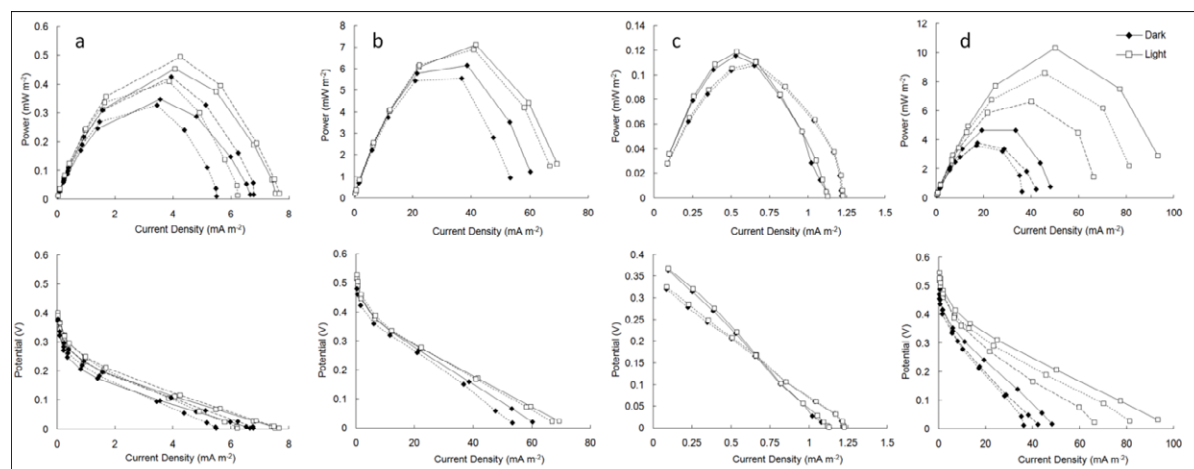
Media	Culture strain	Conductivity (mS)
3N-BBM	<i>Chlorella vulgaris</i>	1.4
Mod F/2	<i>Dunaliella tertiolecta</i>	43.0
BG-11	<i>Synechocystis</i> sp. PCC 6803	2.5
ASW:BG11	<i>Synechococcus</i> sp. WH 5701	43.1
Sea water		40.7
Deionised water		0.002

**Supp. Figure 1.**



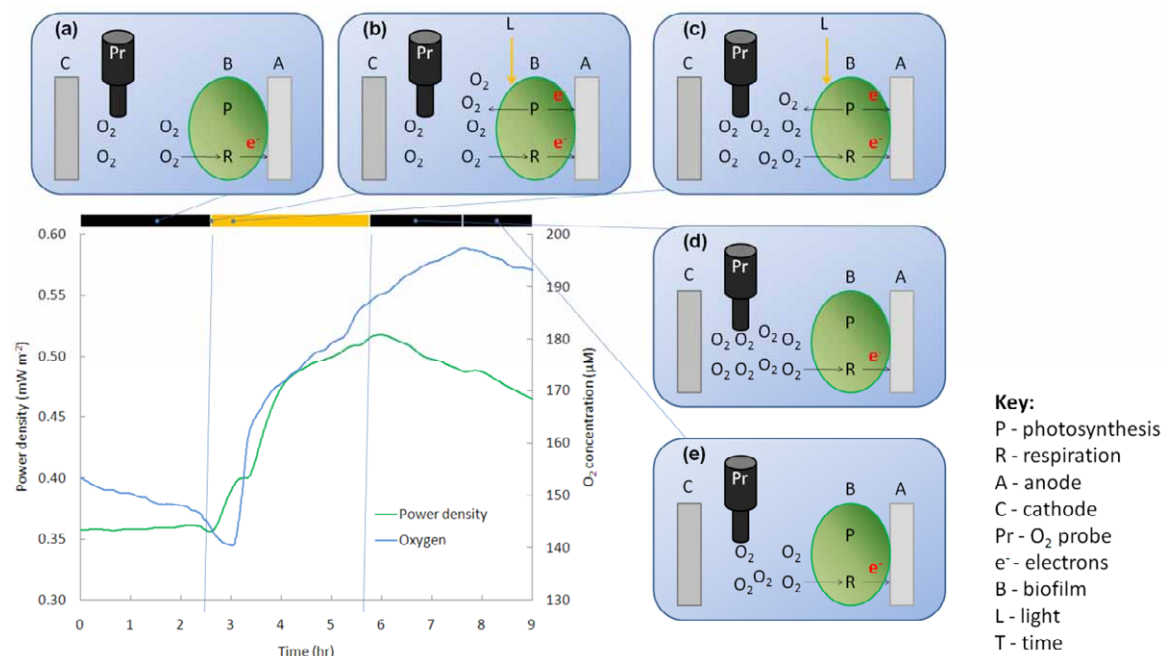
Biofilms following eight days of growth. Photographic (left) and false colour (right) images obtained from confocal fluorescence microscopy are shown for algal and cyanobacterial strains.

**Supp. Figure 2.**



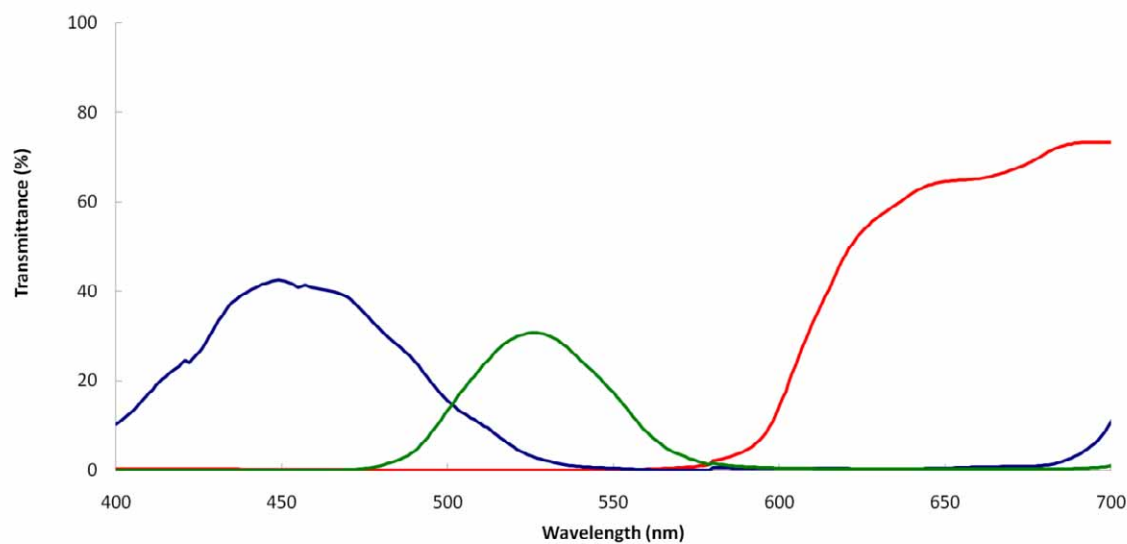
Replicate power curves (top row) and polarization curves (bottom row) of BPV devices with different photosynthetic species. Represented are *C. vulgaris* (a) and *D. tertiolecta* (b) ( $N=2$ ), *Synechocystis* sp. PCC 6803 (c) and *Synechococcus* sp. WH 5701 (d) ( $N=3$ ) under dark (black) and light ( $10 \text{ W m}^{-2}$ ) conditions. Solid, short-dashed and long-dashed lines represent data sets from separate experiments.

Supp. Figure 3.



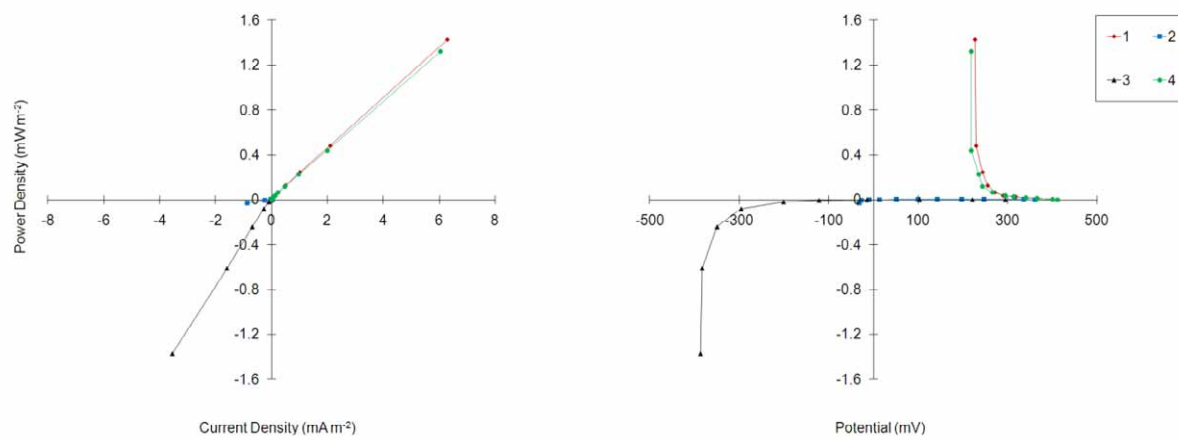
Power outputs and oxygen concentrations in a single-chamber BPV device. An oxygen probe was placed between the anodic biofilm (*Synechococcus* sp. WH 5701) and cathode to allow simultaneous measurements of power outputs and dissolved oxygen concentrations. Prior to illumination (a), oxygen levels decreased due to cellular dark respiration, while power outputs remained constant. Upon illumination ( $10 \text{ W m}^{-2}$ ), power outputs increased (b). After 30 minutes, oxygen levels also increased due to photosynthetic oxygen evolution and delayed diffusion towards the oxygen probe (c). When the light was turned off, power outputs declined, whereas oxygen levels continued to rise (d) before later declining (e). The delay in crossover/diffusion of oxygen evolved during photosynthesis to the probe (and hence the cathode) indicated that the observed light-dependent increases in power outputs are not directly linked to changes in oxygen concentration in the chamber.

**Supp. Figure 4.**



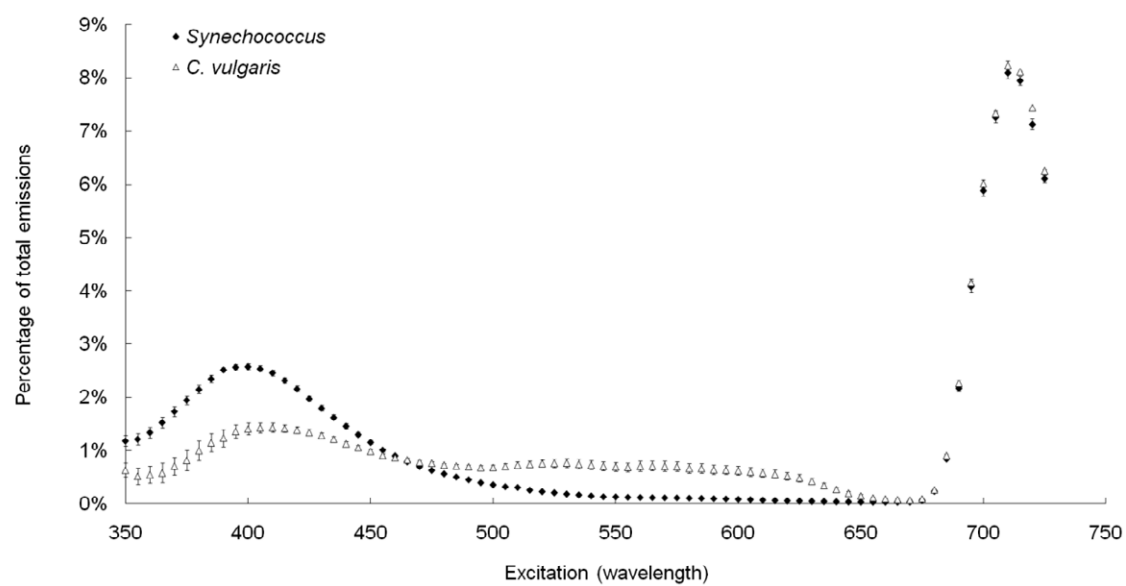
Light filter transmittance for red, blue and green filters. Filters were supplied by Lee Filters Lighting Products, Andover, UK (catalogue numbers #119 [blue], #139 [green] and #106 [red]).

**Supp. Figure 5.**



Performances of four open-air BPVs connected in series. As resistance in the circuit decreased, cells 2 and 3 underwent cell reversal, resulting in the negative potentials (and consequently negative power outputs) observed.

**Supp. Figure 6.**



Loss of light energy through fluorescence for *Chlorella vulgaris* and *Synechococcus* sp. WH 5701. Measurements (N=3) represent the fluorescence emitted over the visible spectrum (370–750 nm) for each species following excitation at the wavelength indicated. The results are presented as a percentage of total emissions over the excitation range measured (350 - 725 nm).